American Journal of Engineering Research (AJER)
e-ISSN: 2320-0847 p-ISSN : 2320-0936
Volume-13, Issue-1, pp-13-26
www.ajer.org
Research Paper Open Access

Developing a Methodology for Creating a Compact Behavioral Models and Expanding the Operating Frequency Range

J. Balaam Alarcón-Angulo[1] & A. Sarmiento-Reyes[1]
[1](INAOE, Puebla, México)
Corresponding Author: jbalan@inaoep.mx & jarocho@inaoep.mx

ABSTRACT : ***This article discusses the development of behavioral compact models for memristive systems. Behavioral compact models are a modelling technique used to describe the behavior of electronic devices in a simple and accurate way. Memristors are electronic devices that can change their resistance based on the electric current flowing through them. These devices have been extensively researched because of their potential to revolutionize electronics. Behaviorally compact models of memristive systems have been explored in recent years due to their ability to describe the behavior of memristive systems in a simple and accurate manner.***
KEYWORDS *Memristor, Memristive System, Macro Model, Filter, Compact Model*

Date of Submission: 01-01-2024 Date of acceptance: 09-01-2024

I. INTRODUCTION

The emergence of memristors has brought forth a new era of electronic exploration, owing to their potential to revolutionize the industry. Memristors, functioning as electronic components, can adjust their resistance based on the electric current passing through them [1]. This distinct characteristic has spurred extensive research on their potential to replicate synaptic activity like that of the human brain, promising a significant shift in electronics. The complexities of memristive systems pose challenges in developing accurate models of their behavior. In recent years, a technique called behavioral compact models has emerged as an effective method of concisely and accurately characterizing memristive behavior.

These models are based on close examination of device behavior, enabling the derivation of a mathematical expression to encapsulate it. In the realm of memristors, the application of behavioral compact models assumes paramount importance, largely because of the inherent complexities of physical modelling.

One prevailing approach to constructing behavioral compact models for memristive systems involves using an equivalent electrical circuit to depict the system's behavior. This approach has been employed to explain memristive systems that range from basic devices to complex multi-layer setups and neural networks. The main limitation of this technique is the possibility of not covering all the intricate aspects of the system. Even though an equivalent circuit could provide a concise and accurate portrayal of the system, it may not comprehensively clarify the fundamental physical processes taking place within it. Attempting to model the system's behavior, especially under difficult conditions or within complicated architectures that have many layers or feedback loops, can result in inaccuracies due to this limitation. As a result, it is of utmost importance to select an appropriate equivalent circuit carefully, ensuring that its accuracy is thoroughly validated through empirical experimentation and simulation.

Moreover, significant progress has been made in developing behavioral compact models that can clarify the behavior of memristive systems across various operational regimes, including both linear and non-linear modes. These models have demonstrated their efficiency in simulating complex memristive systems and predicting their behavior under different circumstances. This article presents a method for obtaining succinct models based on an equation that defines the state variable of a memristive system. This approach is advantageous because the resulting model is useful for both mathematical analysis and simulation purposes.

II. COMPACT MODELLING

In the field of electrical simulation, a compact model pertains to a simplified and effective portrayal of an electronic device or component [2] [3]. Its function is to replicate the component's operation within a bigger

circuit or system, devoid of the necessity to assimilate all the internal intricacies and complexities of the actual device. Compact models embody the fundamental features of a component that are pertinent to applications, facilitating quicker and more manageable simulations.

Typically, these models materialize in the form of mathematical expressions that clarify the component's response to different electrical conditions, such as applied currents and voltages [2] [3]. These concise models offer considerable worth to the design and analysis of electronic circuits, as they enable the effective appraisal of circuit efficiency and behavior before actual manufacturing or implementation of the device.

Memristive systems pose significant challenges for modelling their complex and non-linear behavior using conventional analytical techniques [4] [5]. Therefore, the development of compact models is crucial in describing and comprehending the intricacies of these systems. A compact model provides a simplified portrayal of the system's behavior, capturing its significant features and enabling simulation and analysis.

Recently, various methods have been explored by researchers to create compact models specifically tailored for memristive systems [6] [7]. These methods include behavioral and empirical modelling. Finally, we will maintain an objective and neutral tone throughout. This section will focus on the behavioral modelling approach. Technical abbreviations will be explained when first used. Consistent and standard language, along with clear logical structure, will be employed throughout. Citations and footnotes will also meet the appropriate style guidelines. Efforts will be made to use precise terminology whenever necessary, while avoiding filler words and non-technical terminology. Behavioral models are created by relying on the input-output behavior of the system, using experimental data or simulations to develop their mathematical representations.

We shall explore the basic principles behind behavioral modelling and illustrate how they can be employed to create concise models of memristive systems. Technical terms will be explained on first use, and the text will be free from grammatical errors, spelling mistakes and punctuation errors. We shall employ passive tone and impersonal construction and avoid the excessive use of lists. Quotations will be clearly marked, and filler words being avoided. Our discourse will offer examples of successful use of these principles in memristive systems modelling. We will also ensure a logical flow of information by establishing causal connections between statements. Additionally, we will use formal language devoid of colloquialisms, informal expressions, or biased language.

In the methodology presented **Fig. 1**, we start by selecting a memristive system characterized by an Ordinary Differential Equation (O.D.E.). Our aim is to obtain a concise behavioral model that precisely represents the actions of the memristive system. To accomplish this, we use a systematic method. Next, we proceed to solve the chosen ODE, which will provide us with a crucial component for the following stages of the methodology.

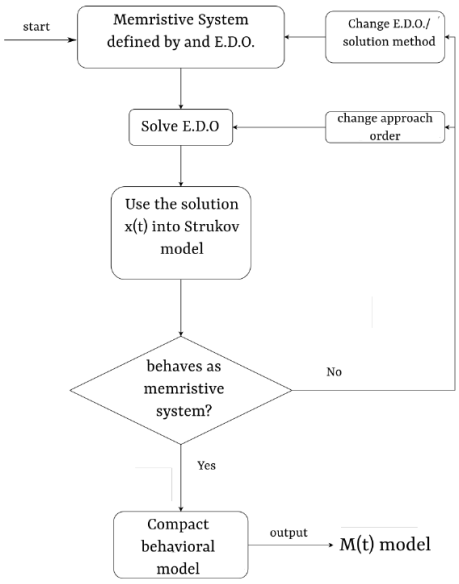

Fig. 1: Methodology to develop compact behavioral memristive model.

Next, we utilize the established Strukov model [2] to describe the memristive behavior. We evaluate whether the model displays the wanted memristive characteristics by merging the acquired solution into the Strukov model. Subsequently, we obtain a condensed behavioral model for the memristive system if the model successfully captures the memristive behavior.

Conversely, in certain scenarios, the primary attempt may not yield a memristive model. In these circumstances, there are two potential courses of action. First, we could adjust the order of the approximation solution to enhance the model's memristive behavior, either increasing or decreasing it. Alternatively, we could alter the technique employed for solving the ODE or investigate alternative solution methods that may give more satisfactory outcomes. After making the required modifications, we proceed to repeat the procedure by integrating the latest solution into the Strukov model and evaluating the resultant model for memristive conduct.

This iterative process persists until a succinct behavioral model successfully represents the characteristics of memristive systems under study. The suggested methodology provides a systematic approach for developing compressed models of such systems, ensuring that the ultimate model encompasses their crucial features. The main aim of the procedure unveiled in **Fig. 1** is to procure a memristive system model characterized by a low computational expense. Such a model is essentially a concise representation of the system's conduct, as it offers a simplified understanding of its behavior. The compact model is based on a viable solution to an O.D.E. that characterizes the memristive system. By carefully choosing a specific solution, a model can be developed that precisely depicts the memristive behavior and has improved computational efficiency.

As a result of its reduced computational complexity, simulators that support the modelling of nonlinear resistors can now feasibly implement the compact model. This methodology permits effective simulation and examination of circuits that integrate memristive systems. The employment of this approach enables us to procure a condensed model that attains a harmonious equilibrium between precision and computational efficiency, rendering it an advantageous asset for circuit design and analysis.

III. Frequency Scaling

One of the challenges encountered by current models, including Biolek [3], Affan [4], TEAM [5], Batas [6], Prodomakis [7], Rak [8], and others, is their dependence on frequency. Such models are restricted in their operational frequency range and encounter performance problems at high frequencies. This constraint is apparent in the fact that the PHL region vanishes as the angular frequency ω approaches infinity [1] .

To tackle this problem, a technique for broadening the frequency range of a memristive system model is illustrated in ***Fig. 2***. The proposed technique permits the customization of pre-existing models to function across a wider range of frequencies. The approach requires modifying the current model to consider higher frequencies through adjusting specific parameters or introducing additional elements. By doing so, it becomes feasible to broaden the frequency range over which the model precisely depicts the behavior of the memristive system.

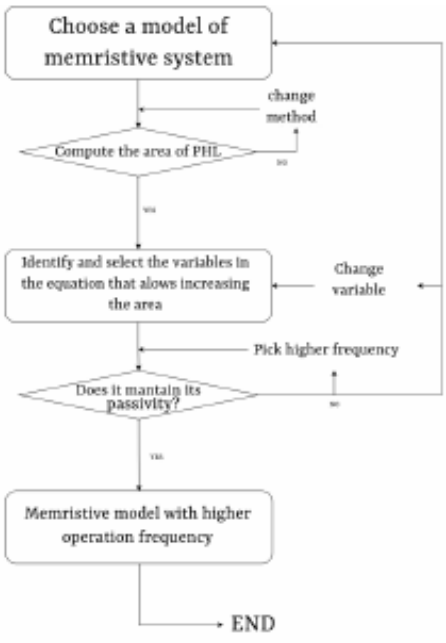

Fig. 2: Methodology to change the operating frequency range of a memristive system model.

By utilizing this approach, it is feasible to surmount the constraints enforced by frequency dependence and construct models that are applicable to a wider array of scenarios, encompassing those encompassing high-frequency signals. Consequently, this permits more extensive and precise scrutinization of memristive systems over a broader frequency spectrum. The process begins by choosing a model and computing its PHL area. If the area can't be obtained, alternative methods are explored. The resulting PHL area value is then scrutinized to identify the factors in the memristive equation that influence its area's increase or decrease. The aim is to examine the impact of these factors on the passivity criterion of the parametric curve.

If the passivity criterion is satisfied by the resulting parametric curve after parameter modification, the model remains within its original frequency range. If, however, the modified curve fails the passivity criterion, this suggests a change in the frequency range has occurred. In such scenarios, selecting a higher frequency value permits the model to meet the passivity criterion once again. This process enables effective frequency range scaling of memristive system models. This facilitates the analysis and simulation of the behavior in these systems over a broader spectrum of frequencies, broadening their potential uses and ensuring precise representation in different frequency regimes.

IV. DEVELOPING A COMPACT MODEL

Fig. *1* illustrates the first step of the methodology, which involves the selection of a memristive system defined by an ODE. The condition that must be satisfied by the state variable of the system is as follows:

$$\dot{x} = \gamma s(t) f_w(x) \qquad (1)$$

where γ represents a relationship between constants i.e., independent variables, $s(t)$ denotes a stimulus signal, and f_w is a window function used to constrain the behavior of the state variable. Table 1 shows that Biolek [3] and Joglekar [9] use a current stimulus $i(t)$, while Affan [8] uses the charge $q(t)$ as stimulus.

Table 1: *Stave-Variable models based on HP memristor.*

Model Name	State Variable	Function Window
Biolek	$\dot{x} = \kappa i(t) f(x)$	$1-(2x-1)^{2p}$
Joglekar	$\dot{x} = \eta\kappa i(t) f(x)$	$1-(2x-1)^{2p}$
Affan	$\dot{x} = \kappa q(t) f(x)$	1

The process begins with the selection of the O.D.E. definition as employed by Biolek, Affan, and Joglekar Table 1. These models utilize the HP memristor equation as a foundation [10], and integrate a window function to adjust its behavior. It is worth noting that all three models conform to the overall structure delineated in Equation (1).

The following step in **Fig. 1** is to discover a resolution to the O.D.E. that includes the state variable. In this case, the homotopic perturbation method (HPM) [11] [12] [13] is employed. This solution is one of many solutions to the HP's memristor equation and is used in the Strukov model \cite{A-HP-1}, resulting in three models (one for each state-variable definition, as shown in Table \ref{T-Models-S_V}). These models capture the time-varying behaviour through the variable $M(t)$ and can be considered as compact models given their representation as one of the multiple solutions derived from the respective state variable equations. The PHL is displayed below.

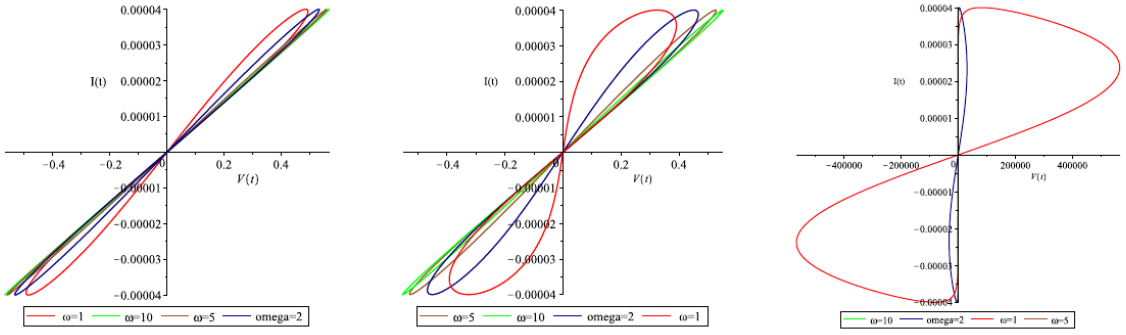

(a) HPM solution of Joglekar state-variable definition. (b) HPM solution of Biolek state-variable definition. (c) HPM solution of Affan state-variable definition.

Fig. 3: PHL of three different models obtained from methodology proposed in Section II.

It can be observed from Fig. 3 that the methodology described in Section II results in a memristive system response [1]. The are of the PHL of Affan (Fig. 3c) exceeds that of the other two. This is due to the window function being equal to one. In contrast, Fig. 3a and Fig. 3b has different shapes in their PHL despite sharing the same window function. The reason for this is that Biolek uses a value of $p = 10$ [3], whereas Joglekar employs $p = 1$ [9].

As anticipated within a memristive system [1], the total area of three PHLs showcased Fig. 3 decreases as frequency increases. This limitation restricts its practical application in high frequency scenarios. By using the methodology described in Section III, it is possible to adjust the operating frequency range. We choose one of the three memristive system models employed to generate the plots of Fig. 3. In this case, Joglekar's O.D.E. model is considered suitable because it displays a smaller PHL, making it easier to observe a modification in its area value.

$$M_{O1_{p=1}} = R_{on}^2 f_w \gamma_1 (\alpha - 1)[\cos \omega t - 1] + R_{init}$$
$$f_w = f_w(X_o)|_{p=1} = 1 - (2X\_o - 1)^{2p}$$
$$R_{init} = [X_o + \alpha(1 - X_o)]R_{on} \quad (2)$$
$$\gamma = {}^{\mu A_p}/_{\Delta^2 \omega}$$

The $M_{O1_{p=1}}$ model comprises an initial resistance value of R_{init}, indicating the device's starting resistance prior to any input signal or stimulus being implemented, and X_o denotes the initial condition of the state variable in the system. It defines the crucial starting value of the state variable, which determines the subsequent evolution and behavior of the memristive system. Both R_{init} and X_o have significant roles in characterising the initial state and behaviour of the memristor in the selected model. After choosing the model for modification of the operation frequency-range, the subsequent step is to ascertain the area of the PHL. This is accomplished by integrating the product of the voltage and current signals within the selected model. The resulting numerical outcome of this integration yields a quantitative measurement of the PHL area, which constitutes a pivotal parameter for scrutinizing the conduct and efficiency of the adapted model. Through analysis of the PHL region, valuable insights can be obtained regarding the characteristics and dynamics of the memristive system under investigation.

$$A_{PHL} = \int_0^{\pi} v(t) i(t) dt \quad (3)$$

By examining the exact time frames of the PHL's commencement and conclusion, a symbolic representation for its area can be derived. For half a period of the input signal $i(t)$, if we consider the voltage signal defined as $v(t) = i(t) M_{O1_{p=1}}(t)$, the integral of the product between the voltage and the current results in an expression that represents the area of the PHL. Equation (3) represents the objective relationship between the input and output variables of the memristive system and measures the PHL area in a quantitative manner.

$$A_{PHL} = \frac{R_{on} A_p^2 ((\alpha - 1)\mu A_p(-1 + (2X_o - 1)\alpha - X_o)\Delta^2 \omega \pi}{2\Delta^2 \omega^2} \quad (4)$$

Equation (4) presents a symbolic expression for calculating the PHL area, which depends on the variables found in Equation (2), used to model a memristive system. It can be observed that the PHL area

decreases in proportion to ω^2, suggesting that the impact of frequency ω can be counterbalanced by appropriately selecting variable values. In this instance, the parameters A_o and X_o are not manipulated due to there are representation of the stimulus signal's amplitude and the initial condition of the state variable $x(t)$, respectively. The variables chosen for alteration are Δ, R_{on}, and μ to observe the model's response during the third stage of scaling the operating frequency depicted in **Fig. 2**. The changing area of the model when the three variables change are shown in Fig. 4, the frequency for the analyses was $1Hz$. This examination yields valuable insights into the correlation between the parameter values and the resulting PHL area.

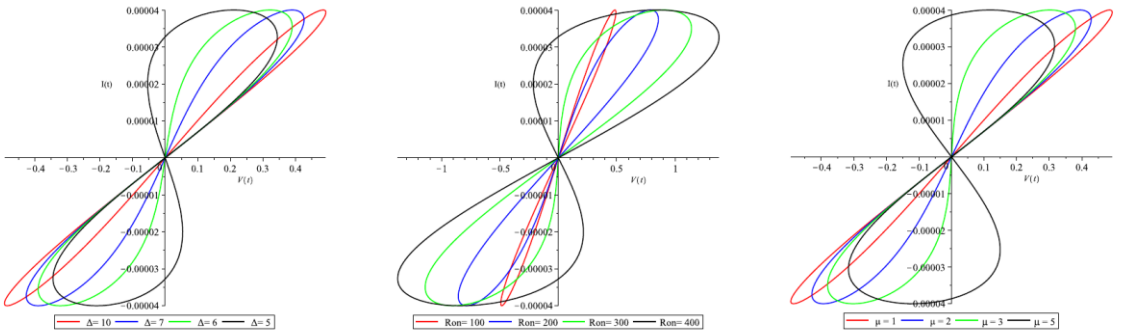

(a) PHL when Δ changes, each value is by 10^{-9}. (b) PHL when R_{on} changes. (c) PHL when μ changes, each value is by 10^{-14}.

Fig. 4: Modification of the numerical value of three variables in memristor model of Joglekar.

The influence of altering the values of the variables Δ, R_{on}, and μ on the area of the PHL is illustrated by Fig. 4. It is apparent that the PHL expands with an increase in these variables. Table 2 denotes the specific values of Δ, R_{on}, and μ. However, it is worth noting that once the PHL area exceeds a specific threshold, specified by the black PHL curve in Fig. 4, the model no longer demonstrates the characteristics of a memristive system and fails to satisfy the passivity criterion [1], allowing the increase in the operation frequency-range making that model meets the passivity criterion again, and Thus, the frequency range of the memristive device can be expanded.

Table 2: Values of maximum and minimum memristance, and te area of Joglekar model.

	Max	Min	Area
$\Delta_{red} = 10 \times 10^{-9}$	$14.41K\Omega$	$9.83K\Omega$	3.0461×10^{-5}
$\Delta_{blue} = 7 \times 10^{-9}$	$14.41K\Omega$	$5.06K\Omega$	2.4473×10^{-5}
$\Delta_{green} = 6 \times 10^{-9}$	$14.41K\Omega$	$1.69K\Omega$	2.0231×10^{-5}
$\Delta_{black} = 5 \times 10^{-9}$	$14.41K\Omega$	$-3.9K\Omega$	1.3199×10^{-5}
$R_{on_{red}} = 100$	$14.41K\Omega$	$9.83K\Omega$	3.0461×10^{-5}
$R_{on_{blue}} = 200$	$28.82K\Omega$	$10.5K\Omega$	2.4473×10^{-5}
$R_{on_{green}} = 300$	$43.23K\Omega$	$2.01K\Omega$	2.0231×10^{-5}
$R_{on_{black}} = 400$	$57.64K\Omega$	$-15.63K\Omega$	1.3199×10^{-5}
$\mu_{red} = 1 \times 10^{-14}$	$14.41K\Omega$	$9.83K\Omega$	3.0461×10^{-5}
$\mu_{blue} = 2 \times 10^{-14}$	$14.41K\Omega$	$5.25K\Omega$	2.4473×10^{-5}
$\mu_{green} = 3 \times 10^{-14}$	$14.41K\Omega$	672.4Ω	2.0231×10^{-5}
$\mu_{black} = 5 \times 10^{-14}$	$14.41K\Omega$	$-8.49K\Omega$	1.3199×10^{-5}

Table 2 presents the values for the three adaptable parameters, namely Δ, R_{on}, and μ, alongside the corresponding area values of the PHL. Furthermore, the maximum and minimum values of Equation (2) are included for reference purposes. These values serve as crucial indicators for comprehending the conduct and traits of the memristive system. The variable names with color subscripts are displayed in the first column of Table 2, clarifying the association between the variable values and their corresponding PHL curves in Fig. 4 and Fig. 5.

The second column displays the highest memristance value attained from Equation (2), at $t = 0$. It is important to note that the maximum memristance remains consistent irrespective of any variations in the

variables Δ and μ. The third column indicates the lowest memristance value obtained from Equation (2), occurring at $t = N\pi/\omega$, $N = 0,2,4 \ldots, \infty_{EVEN}$. Typically, the minimum memristance value declines as the variable values change, except when $R_{on} = 200\Omega$. This behaviour may be attributed to the fact that the memristance value at any given time is determined by the derivative $d(PHL(t))/dt$, and the minimum value occurs when $t = N\pi/\omega$, $N = 1,3,5 \ldots, \infty_{ODD}$.

The fourth column displays the PHL area values for each variable value. The results reveal that as Δ and R_{on} increase, the PHL area generated by Equation (2) also increases, while decreasing μ leads to a rise in the area. Table 2 demonstrates the relationship between the variable values and their impact on the memristance behavior, along with the corresponding PHL area. If the area of the PHL cannot be calculated directly, another approach is to analyze the output signal of the memristive system, in this model is the voltage. Fig. 5 offers valuable insights into the behavior of the output voltage, providing a valuable perspective on the system's response.

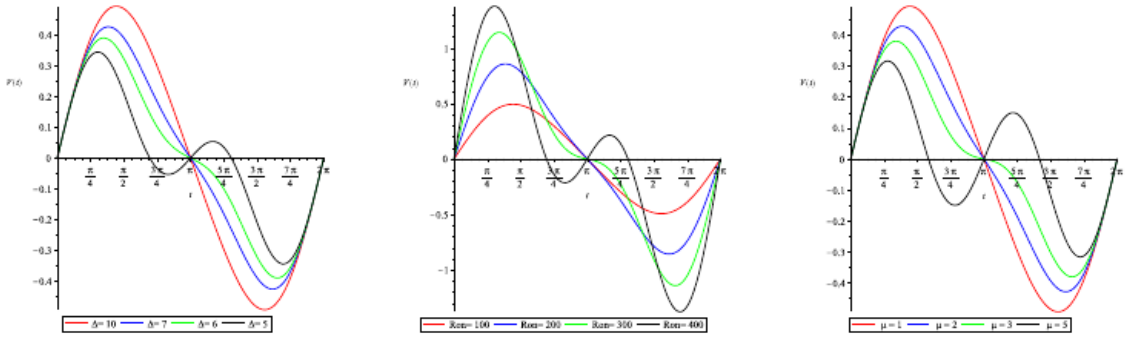

(a) Output signal when Δ changes, each value is by 10^{-9}. (b) Output signal when R_{on} changes. (c) Output signal when μ changes, each value is by 10^{-14}.

Fig. 5: Voltage behavior when the variables are changed.

The black line in the diagrams displays the point at which the model no longer shows passive device behavior. This phenomenon is apparent through the double valley/peak patterns detected in all three instances. When the model displays the double valley/peak pattern, the operation frequency can be increased. This, in turn, results in the system modelled by Equation (2) operating at a higher frequency. Fig. 4 and Fig. 5 provide the necessary information to obtain a memristive model with higher operation frequency in Section III.

If the passivity criterion is satisfied by the resulting parametric curve after parameter modification, the model remains within its original frequency range. If, however, the modified curve fails the passivity criterion, this suggests a change in the frequency range has occurred. In such scenarios, selecting a higher frequency value permits the model to meet the passivity criterion once again. This process enables effective frequency range scaling of memristive system models. This facilitates the analysis and simulation of the behavior in these systems over a broader spectrum of frequencies, broadening their potential uses and ensuring precise representation in different frequency regimes.

V. IMPLEMENTATION OF THE DEVELOPED MODEL

The memristive system model of Joglekar, has been implemented in a hardware security system [14]. This Section illustrates that the models obtained from the methodologies proposed in this paper have potential for use in multiple applications. Additionally, memristive devices have demonstrated significant potential in improving the performance of electronic filters [15] [16] [17]. Compared to conventional filters, memristive filters provide several benefits such as nonlinearity, tunability, and compactness. The implied nonlinearity of memristive devices can be effectively employed to accomplish higher-order filtering functions, which are inherently hard to achieve through linear filters [18]. Moreover, the adjustability of memristive devices permits precise frequency selectivity and parameter modifications, making them ideally suited for adaptive filtering applications [19]. Furthermore, the compact size of memristive devices allows for the creation and integration of smaller and more efficient filters, making them well-suited for use in portable and wearable devices [20].

As seen previously, the integration of memristive devices into filters shows great potential for creating high-performance filters that offer adjustable frequency responses and multiple filter outputs using a single

circuit topology. This section will detail the design and simulation process of a memristive state-variable filter, emphasizing its aptitude for communication systems and biomedical signal processing applications.

A. Designing a state-variable memristive filter

A state variable memristive filter uses the ability of a memristive system to change its resistance in adjust dynamically the parameters of the filter, which is a distinctive characteristic in signal processing application, one of these parameters is the quality factor Q. As we know, the quality factor is a parameter used in the characterisation of filters, since its value affects the efficiency and selectivity. A high Q value indicates a more selective filter, while a low Q value indicates a less selective bandwidth. Therefore, we start with the definition $Q = f_o/B_w$ of a state variable filter, where f_o is the cut-off frequency, and B_w is the bandwidth. If all the devices in Fig. 6 are linear, the quality factor can be calculated as:

$$Q = \frac{R_1(R_3 + R_4)}{R_4(R_1 + Z_{eq})}\sqrt{\frac{R_3 RC}{R_4 RC}} \qquad (5)$$

where $Z_{eq} = R_2 + Z_M$, considering Z_M as an impedance. If $R_3 = R_4$ then Equation (5) can be simplified to $Q = 2R_1/R_1 Z_{eq}$, this approximation can be used in the filter shown in Fig. 6 when Z_M is a memristive system and allows to its instantaneous resistance [4].

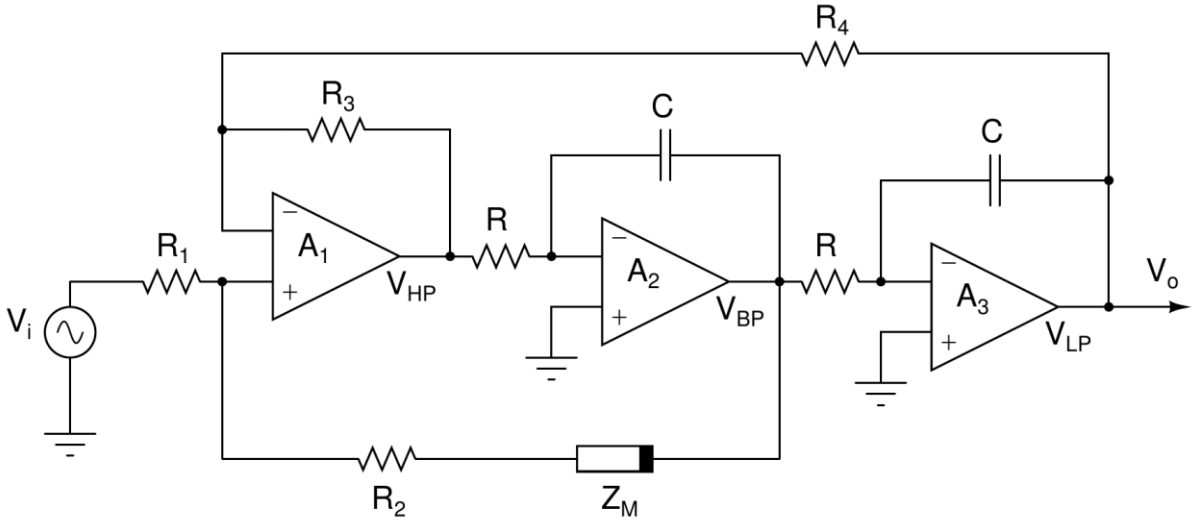

Fig. 6: State-Variable Memristive-Filter, which the memristive element Z_m is modeled using Equation (2).

The memristive feedback for band-pass stage is formed by two elements of the ohmic class [21] R_2 and Z_M. Resistors R and Capacitors C have the same value. With these considerations in mind, we can study the dynamic changes in the filter's quality factor over time. The gain, which is influenced by the memristive feedback, plays a key role in determining the filter's response to different types of signals and in assessing the overall stability of the system. Bearing in mind that Z_M oscillates between its max/min values (Table 2), causing that Z_{eq} also has two values, and therefore the quality factor Q also has two values. To simplify the calculations, we assume that V_i is a periodic signal, making that Z_{eq} oscillates between its max/min values.

$$Z_{eq}(t) = R_2 + \begin{cases} Z_{M|_{max}}(t) & t = {a\pi}/{\omega} \quad a = 1,3,\dots,N \\ Z_{M|_{min}}(t) & t = {b\pi}/{\omega} \quad b = 0,2,4,\dots,M \end{cases} \qquad (6)$$

The value of R_2 is chosen in base of the current control value of memristive element Z_M , which is modeled by Equation (2), and using the same parameter values that are used on HP memristor [10], then Z_M ssumes two distinct values: $Z_{M|_{max}} = 14.41K\Omega$ at $t = 0$, and $Z_{M|_{min}} = 1.69K\Omega$. To gain deeper insights into the system's behavior, we will conduct simulations of the modified circuit using the software tool *Analog Insides* and subsequently analyze the obtained results. Let us define the quality factor, denoted now as $Q(t)$, for the state-variable filter shown in Fig. 6, this definition considers the presence of the memristive system Z_M, which introduces time-varying impedance values. The quality factor is defined as:

$$Q(t) = \frac{2R_1}{R_1 + Z_{eq}} \qquad (7)$$

If Equation (6) is substituted into Equation (7), the result is:

$$Q(t)_{|_{t=a\pi/\omega}} = \frac{2R_1}{R_1 + (R_2 + Z_{M|_{max}})}$$
$$Q(t)_{|_{t=b\pi/\omega}} = \frac{2R_1}{R_1 + (R_2 + Z_{M|_{min}})} \quad (8)$$

When $Z_{eq}(t)$ was composed only by linear elements and we fixed the impedance in $19K\Omega$, and $R_1 = 1K\Omega$, the state-variable memristive-filter in Fig. 6 has a quality factor of 0.1. Using Equation (7) is possible to appreciate that $Q(t)$ increase when Z_{eq} decrease. With the above in mind, it is possible to make the analyses when Z_M, contained in Z_{eq}, is a memristive system. Equation (2) allows to obtain its Z_{max} value in the initial condition $t = 0$, in this condition the feedback Z_{eq} shows its maximum value, allowing to calculate R_2

$$R_2 = Z_{eq} - Z_{M|_{max}} \quad (9)$$

The above equation is a valuable tool in determining the appropriate value for the support resistor R_2. Substituting $Z_{M|_{max}}$ (see Table 2), and $Z_{eq} = 19K\Omega$ which is the condition for having a quality factor of $Q(t_{|=0}) = 0.1$, we obtain a that $R_2 = 4.59K\Omega$, the value is approximate to a commercial value of $4.6K\Omega$.

Table 3: Values of R_2, $Q(t)$, and corresponding $Z_{M|_{max}}$.

Q(t)	R_2	$Z_{M|_{max}}$
0.1~0.3	$4.6K\Omega$	$14.41K\Omega$
0.5~0.9	$1K\Omega$	$2.06K\Omega$
0.9~1.5	200Ω	$1.03K\Omega$

The result of introducing a memristive element $Z_{M|_{max}}$ into the positive feedback of the filter in Fig. 6, is a periodic time-dependent quality factor $Q(t)$ that oscillates between two values, as can be seen in the first column of Table 3. Each row in the table corresponds to a different condition of Z_M. The second column shows Equation (9) evaluated for three values of Z_{eq}; $19K\Omega$, $3K\Omega$, and $1.2K\Omega$, and $Z_{M|_{max}}$ is modelled by Equation (2), with the same conditions as Δ_{green} in Fig. 4 and evaluated at $t = 0$. Values of the Equation (2) shown in Table 2 reveal that the maximum value reached is $14.41K\Omega$, therefore the third column in Table 3 shows three different values for $Z_{M|_{max}}$, this is possible thanks to Z_M being a parallel memristor arrangement in two cases, the equivalent resistance is obtained by:

$$Z_{M|_{parallel}} = \frac{1}{\frac{1}{M_a(t)} + \frac{1}{M_b(t)} + \cdots + \frac{1}{M_k(t)}} \quad (10)$$

if $M_a(t) = M_b(t) = \cdots = M_k(t)$, then the above equation can be reduced to:

$$Z_{M|_{parallel}} = \frac{M(t)}{k} \quad (11)$$

where $M(t)$ is modelled by the equation (2) and k represents the number of elements connected in parallel, which is possible when the circuit has an ohmic class element [21]. Fig. 7 shows the impulse response of the state-variable filter under two different scenarios: one is when all passive elements in the filter are linear (green curve), and the other scenario is when $Z_M$is a memristive system (red curve). The simulation was done with *Analogue Insides*.

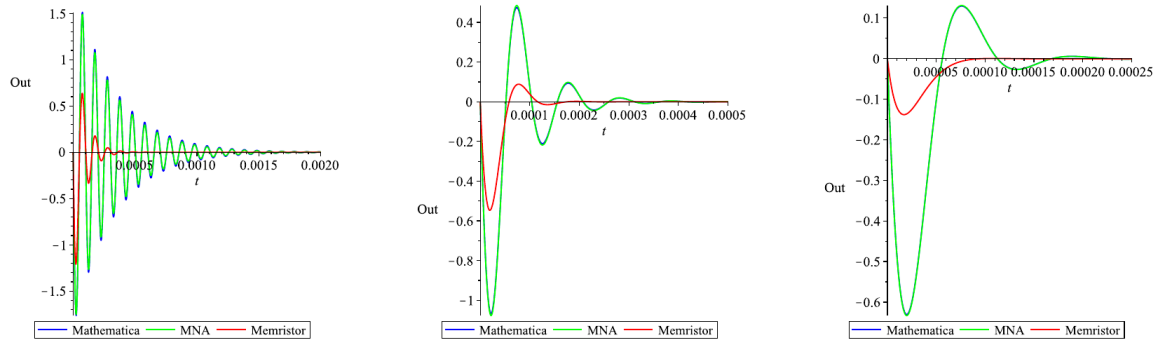

(a) Filter response when $Z_{eq} = 19K\Omega$.

(b) Filter response when $Z_{eq} = 3K\Omega$.

(c) Filter response when $Z_{eq} = 1.2K\Omega$.

Fig. 7: Response to impulse from a state-variable filter. In one scenario Z_M is a lineal resistor (green line), in other scenario, is a memristive system (red line).

Six study cases are shown in Fig. 7, the green curve is the response of the filter for three values of Q, 0.1, 0.5, and 0.9. The red curve is the response of the filter when $Q(t)$ takes the values shown in Table 3. We can see that the memristive filter (red curve) reaches stability in $1/3$ of time, compared to the linear filter (green curve). Applications that require a fast response and a fast transition to a new state show a better performance when containing a memristive system. The speed in the response of the filter to disturbances in the input signal, is not the only benefit of Z_M, if we see the $V_{pp_{max}}$ reached by the filter in Fig. 7, when the memristive system is present the overshoot is reduced by 2. Reducing the overshoot magnitude generates; less stress in the elements and improves the signal quality.

Fig. 7 shows that the model generated using the methodology proposed in section II can be used in the *AnalogInsydes* simulator and allows the mathematical analyses, both essential in electronic design. In reference to filter design, obtaining the stability of the system is useful, one method to know if a system is stable is to analyses its poles and zeros graphs.

B. Poles and Zeros

In the realm of filters, the concepts of poles and zeros are of great importance in understanding the frequency response of a system. Poles and zeros manifest themselves as points within the complex plane and provide valuable insight into the inherent characteristics of the filter. Poles are defined as the frequency values at which a filter's response diverges to infinity or approaches zero. They represent the frequencies at which the system exhibits maximum sensitivity or resonance. The presence of poles plays a crucial role in shaping and determining the characteristics of the filter's frequency response. Zeros, on the other hand, correspond to the frequencies at which a filter's frequency response is null or zero. They are the frequencies at which the system does not respond or effectively suppresses certain components of the input signal. Zeros play a crucial role in shaping the behavior and characteristics of the filter and have a significant impact on its overall performance.

The positions of the poles and zeros within the complex plane play a crucial role in shaping and defining the characteristics of a filter. Fig. 8 visually illustrates the varied placement of Poles and Zeros across the complex plane, covering both the left half of the plane. The strategic distribution and configuration of the poles and zeros has a significant effect on the resulting frequency response and overall stability of the filter.

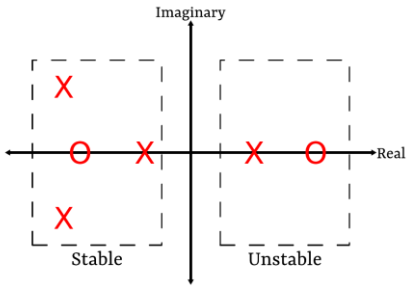

Fig. 8: Poles and Zeros to the left, the system is stable, and when they on the right side of the plane the system is unstable.

Fig. 8 shows the distribution of poles and zeros for both stable (left) and unstable (right) systems. Techniques used in the field of state variable filters to determine these locations include the diagonalization method, stability analysis, Laplace transform and parametric design. The diagonalization method focuses on transforming the state coefficient matrix into a diagonal form, allowing poles and zeros to be extracted directly from the matrix elements. Stability analysis, which is crucial for pole determination, examines the state coefficient matrix to assess system stability by evaluating the real parts of the poles. The Laplace transform, a fundamental tool, derives the transfer function and helps to identify poles and zeros from the characteristic polynomial roots.

In addition, parametric design defines filter characteristics through parameters such as cut-off frequency. By optimizing these parameters, poles and zeros can be precisely located, allowing filter designs to be tailored to specific requirements. Together, these methods provide a systematic approach to modelling and controlling filter behavior, ensuring optimized performance for a wide range of applications. These techniques are among the most widely used in the analysis and design of state-variable filters.

By including a memristive elements in the analysis, we can explore the impact of their unique properties on the behavior and performance of state-variable filter. This approach opens new possibilities in filter design and provides valuable insights into the benefits and challenges of integrating memristive elements into practical applications. To determine the poles and zeros of the system shown in Fig. 6, we start defining its transfer function.

$$H(s) = \frac{V_{Bp}}{V_i} = H_o \frac{\frac{s}{Q\omega_0}}{(\frac{s}{\omega_0})^2 + \frac{s}{Q\omega_0} + 1} \quad (12)$$

where H_o is the gain of filter, and ω_0 is the cut off frequency. To determine the poles the denominator is evaluate for a value $Q = 0.1$, obtaining:

$$-28127.73 \pm 55812.89I \quad (13)$$

By evaluating the denominator of $H(s)_{|Q=0.1}$, we note the presence of two poles. Complementing the poles, we can also determine the zeros of the system by looking at the numerator of the transfer function. The zero is obtained:

$$-0.00625 \quad (14)$$

The system represented by Fig. 6 exhibits one Zero value, when all the passive elements are lineal devices. The positions of the Poles and Zeros are depicted in the S-plane by plotting the values Equations (13) and (14).

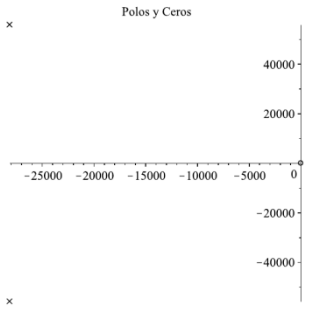

Fig. 9: Poles and Zeros of the state-variable filter with lineal passive elements.

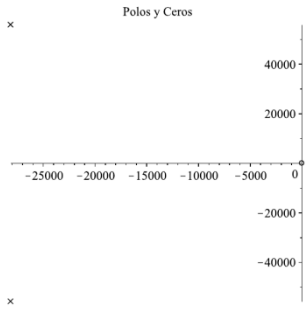

Fig. 9 shows the distribution of poles and zeros for typical state-variable filter. The poles are to the left of the S-plane, this means that all frequencies causing divergence are confined to this area. This characteristic indicates that the system is stable as there are no infinite responses at any frequency when $Q = 0.1$. For obtain poles and zeros of a state-variable memristive-filter i.e., Z_M in Fig. 6 is a memristive device. To obtain the transfer function we use the MNA stamps, assuming Z_M as an ohmic element. To solve the matrix, we use the diagonalization technique [22] [23], and the resulting node voltage V_{BP} is used to obtain its transfer function, and finally we obtain the poles and zeros.

Table 4: Poles and zeros of the state-variable memristive-filter

Poles	Zeros
$P_1 = 0$	$Z_1 = 0$
$P_2 = 10 \times 10^3 I$	$Z_2 = -6.25 \times 10^{-3}$
$P_3 = -10 \times 10^3 I$	$Z_3 = 10 \times 10^3 I$
$P_4 = -129.38 \times 10^{-3} + 10.4 \times 10^3 I$	$Z_4 = -10 \times 10^3 I$
$P_5 = -52.08 \times 10^3 + 34.55 \times 10^3 I$	$Z_5 = -834.40 \times 10^{-3} + 9.99 \times 10^3 I$
$P_6 = 579.61 \times 10^{-3}$	$Z_6 = -3.48$
$P_7 = -52.05$	$Z_7 = -834.40 \times 10^{-3} - 9.99 \times 10^3 I$
$P_8 = 129.38 \times 10^{-3} - 10.04 \times 10^3 I$	

Table 4 gives the specific values for the system's poles and zeros, giving precise information about their frequencies. These values are of paramount importance in analyzing and understanding the behavior and characteristics of the state-variable memristive-filter. To aid understanding and visualization, the corresponding poles and zeros are plotted graphically. It is evident that the inclusion of a non-linear element in the system leads to the appearance of additional poles and zeros. This phenomenon is illustrated in the following figure.

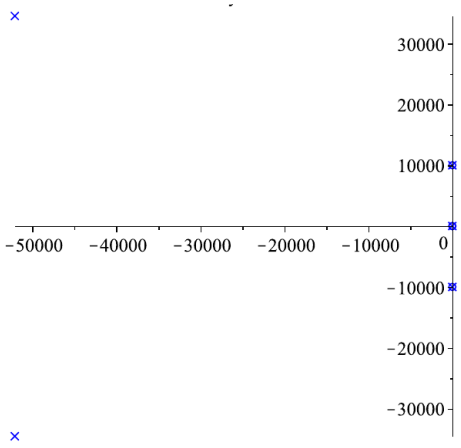

Fig. 10: Poles and zeros of a state-variable memristive-filter.

Fig. 10 displaying a distinct Poles and Zeros at the origin, this indicates that the system's response frequency becomes zero at the zero-frequency point and results in a 180° phase shift. Consequently, the system can effectively reject signals at zero frequency, thereby contributing to its frequency-selective behavior. Additionally, two Poles and two Zeros are situated along the imaginary axis. This attribute signifies that the system's frequency response wholly fluctuates with imaginary frequencies, the existence of these Poles and Zeros causes oscillations or resonances within the system, which illustrates their important function in shaping the system's performance at certain frequency components. Finally, two additional Poles on the left side of the complex plane, showing us the frequency at which system's response decay exponentially, indicating that system can reach a steady state, this stability characteristic is of utmost importance for ensuring the reliable and predictable operation of the system.

Poles and zeros analyses demonstrate that the implementation of a memristive system results in an increase in the quality factor, as illustrated in Table 3. The real-time dynamic adjustment of the quality factor Q has valuable applications in various contexts. In wireless communications, it enables the filter to adapt to changing channel conditions, enhancing selectivity and spectral efficiency. In audio and signal processing systems, the aim is to optimize the filter response for variable acoustic conditions. Control systems require dynamic Q adjustments to respond to sudden changes in system conditions. RF electronics, image processing instrumentation, and sensor networks can benefit from real-time, selective filter response improvements that adapt to changing application needs, ultimately maximizing system performance.

VI. CONCLUSION (10 BOLD)

The proposed methodology for obtaining a streamlined behavioral model and changing the operational frequency range in a memristive system can generate a minimum of three concise models. One of the generated models was employed to create a state-variable memristive filter, which exhibited superior performance compared to a system with similar impedance characteristics but without a memristive system. Furthermore, the same model and parameters used in the state-variable memristive-filter were employed to analyze low computational cost and other applications.

Having a variety of compact models that function in various applications and exhibit diverse behaviors in their PHL can be beneficial for computed-aided design (CAD) because it enables the development of memristive system libraries that can serve in different circuit applications. This approach also provides different operational working conditions between models, namely the maximum/minimum memristance and the operation frequency range.

REFERENCIAS

[1]. L. O. Chua y S. M. Kang, «Memristive devices and systems,» Proceedings of the IEEE, vol. 64, nº 2, pp. 209-223, 1976.
[2]. D. B. Strukov, G. S. Snider, D. R. Stewar y R. S. Williams, «The missing memtitor found,» Nature, vol. 453, pp. 80-83, 2008.
[3]. Z. Biolek, D. Biolek y V. Biolkova, «Spice model of memristor with nonlinear dopant drift.,» Radioengineering, vol. 18, nº 2, 2009.
[4]. a. M. A. Z. a. K. S. A. G. Radwan, «Hp memristor mathematical model for periodic signal and dc,» 2010 53rd IEEE International Midwest Symposium on Circuits and Systems, pp. 861-864, 2010.
[5]. a. E. G. F. a. A. K. a. U. C. W. S. Kvatinsky, «Team: Threshold adaptive memristor model,» IEEE transactions on circuits and systems I: regular papers, vol. 60, nº 1, pp. 211-221, 2012.
[6]. a. H. F. D. Batas, «A memristor spice implementation and a new approach for magnetic flux-controlled memritor modeling.,» IEEE Transactions on Nanotechnology, vol. 10, nº 2, pp. 250-255, 2010.
[7]. a. B. P. P. a. C. P. a. C. T. T. Prodomakis, «A versatile memristor model with nonlinear dopand kinectics.,» IEE transactions on electron devices, vol. 58, nº 9, pp. 3099-3150, 2011.

[8]. a. G. C. A. Rak, «Macromodeling of the memristor in spice,» IEEE Transactions on Computer-Aided Design of Integrated Circuits and Systems, vol. 29, nº 4, pp. 632-3636, 2010.
[9]. Y. N. Joglekar y S. J. Wolf, «The elusive memristor: properties of basic electrical circuits.,» European Journal of Physics, vol. 30, nº 4, pp. 661-675, 2009.
[10]. a. Y. S. K. a. A. .. T. a. K. E. a. S. F. A.-S. a. D. A. O. Kavehei, «The fourth element: Insights into the memristor,» de 2009 IEEE Internationl Conference on Communications, Circuits and Systems, 2009.
[11]. J. B. A.-A. Arturo Sarmiento-Reyes, «Nullor-Based Negative-Feedback Memristive Amplifiers: Symbolic-Oriented Modelling and Design,» de Pathological Elements in Analog Circuit Design, Springer, 2018, pp. 329-360.
[12]. J. H. He, «Homotopy perturbation method: a new nonlinear analytical technique.,» Applied Mathematics and computation, vol. 135, nº 1, pp. 73-79, 2003.
[13]. H. Vazquez-Leal, «Generalized homotopy method for solving nonlinear differential equations.,» Computational and Applied Mathematics, vol. 33, nº 1, pp. 275-288, 2014.
[14]. a. S.-R. A. Alarcon-Angulo J. Balaam, «A high frequency memristor model applied to hardware security.,» American Journal of Engineering Research (AJER), vol. 12, nº 5, pp. 01-12, 2023.
[15]. a. G. S. a. F. Q. a. C. W. a. S. W. R. Lin, «Research progress and applications of memristos emulator circuits.,» Microelectronics Journal, p. 105702, 2023.
[16]. a. H. X. X.-B. Tian, «The design and simulation of a titanium oxide memristor-based programmable analog filter in a simulation program with integrated circuit emphasis,» Chinese Physics B, vol. 22, nº 8, p. 088501, 2013.
[17]. a. S. S. A. a. R. R. a. R. V. Vishnu S., «Application of memristores in active filters,» de 2016 3rd International Conference on Devices, Circsuits and Systems (ICDCS), 2016.
[18]. a. H. C. a. K. L. P. a. W. R. S. a. P. S. Korkmaz A., «Design of tunable analog filters using memristive crossbars.,» 2021 IEEE International Symposium on Circuits and Systems (ISCAS), pp. 1-5, 2021.
[19]. a. Q. J. a. K. S. a. K. H.-T. a. K. B. a. P. V. V. D. M. a. B. D. Driscoll T., «Memristive adaptive filters,» Applied Physics Letters, vol. 97, nº 9, p. 093502, 2010.
[20]. a. B. M. a. M. P. Shah J., «Memristor crossbar memory for hybrid ultra low power hearing aid speech processor.,» 2013 13th IEEE International Conferenco on Nanotechnology, pp. 83-86, 2013.
[21]. W. F. Z., «A triangular table of elementary circuits elements.,» IEEE Transactions on Circuits and Systems I: Regular Papers, vol. 60, nº 3, pp. 616-623, 2013.
[22]. F. a. T. F. L. a. D. V. M. Caravelli, «Complex dynamics of memristive circuits: Analytical results and universal slow relaxation.,» Physical Review, vol. 95, nº 2, p. 022140.
[23]. R. Vollgraf and K. Obermayey, «Quadratic optimization for simultaneous matrix diagonalization,» IEEE Transactions on Signal Processing, vol. 54, nº 9, pp. 3270-3278, 2006.
[24]. D. A. Neamen, Microelectronics: circuits analysis and design, New York: McGraw-Hill, 2007.
[25]. M. H. Rashid, Spice for porwer electronics and electric power., CRC press, 2005.